Effect of Lysine Side Chain Length on Intra-Helical Glutamate−Lysine Ion Pairing Interactions†

Richard P. Cheng,* Prashant Girinath, and Raheel Ahmad

Department of Chemistry, University at Buffalo, The State University of New York, Buffalo, New York 14260-3000

Received April 13, 2007

ABSTRACT: Ion-pairing interactions are important for protein stabilization. Despite the apparent electrostatic nature of these interactions, natural positively charged amino acids Lys and Arg have multiple methylenes linking the charged functionality to the backbone. Interestingly, the amino acids Lys and Orn have positively charged side chains that differ by only one methylene. However, only Lys is encoded and incorporated into proteins. To investigate the effect of side chain length of Lys on ion-pairing interactions, a series of 12 monomeric α-helical peptides containing potential Glu−Xaa (*i*, *i*+*3*), (*i*, *i*+*4*) and (*i*, *i*+*5*) (Xaa = Lys, Orn, Dab, Dap) interactions were studied by circular dichroism (CD) spectroscopy at pH 7 and 2. At pH 7, no Glu−Xaa (*i*, *i*+*5*) interaction was observed, regardless of the Xaa side chain length. Furthermore, only Lys was capable of supporting Glu−Xaa (*i*, *i*+*3*) interactions, whereas any Xaa side chain length supported Glu−Xaa (*i*, *i*+*4*) interactions. Side chain conformational analysis by molecular mechanics calculations showed that the side chain length of Lys enables the Glu−Xaa (*i*, *i*+*3*) interaction with lower energy conformations compared to residues with side chain lengths shorter than that of Lys. Furthermore, these calculated low energy conformers were consistent with conformations of intra-helical Glu−Lys salt bridges in a non-redundant protein structure database. Importantly, the CD spectra for peptides with Glu−Lys interactions did not alter significantly upon changing the pH because of a greater contribution to these interactions by forces other than electrostatics. Incorporating side chains just one methylene shorter (Orn) resulted in significant pH dependence or lack of interaction, suggesting that nature has chosen Lys to form durable interactions with negatively charged functional groups.

Electrostatic ion-pairing interactions are prevalent in many biological inter and intramolecular interactions. In particular, ion pairs occur frequently in protein structures (*1*−*3*). Such attractive electrostatic interactions between oppositely charged amino acids have been shown to stabilize proteins (*4*, *5*). Furthermore, optimized electrostatic profiles (charged networks) on protein surfaces have been observed in thermophilic proteins (*6*−*13*). Because of the importance of electrostatic interactions in protein stability, the energetics of individual salt bridges have been determined in proteins. Salt bridges are hydrogen-bonded ion pairs (*14*, *15*). Buried salt bridges can contribute up to 5 kcal·mol^{-1} stabilization (*16*−*18*), whereas surface salt bridges can contribute up to 1 kcal·mol^{-1} (*19*−*23*). Interestingly, natural positively charged residues lysine (Lys) and arginine (Arg) have side chains with multiple methylenes linking the charged functionality to the backbone (Chart 1). Since the positively charged functionality constitutes the electrostatic component for ion-pairing interactions, the role played by the linking methylenes in ion-pairing interactions remains unclear. Furthermore, it may be more logical for nature to employ ornithine (Orn), which is one methylene shorter than Lys rather than Lys, on the basis of biosynthetic availability. Orn is synthesized by all organisms as an intermediate for the Arg biosynthesis from glutamate (Glu), while lysine (Lys) is synthesized from aspartate (Asp) only by plants and bacteria. However, Lys is encoded and incorporated into natural proteins, whereas Orn is not.

Chart 1: Chemical Structures of the Positively Charged Residues Ornithine (Orn), Lysine (Lys), and Arginine (Arg) and the Corresponding Intramolecular Side Chain to Backbone Cyclic Lactams

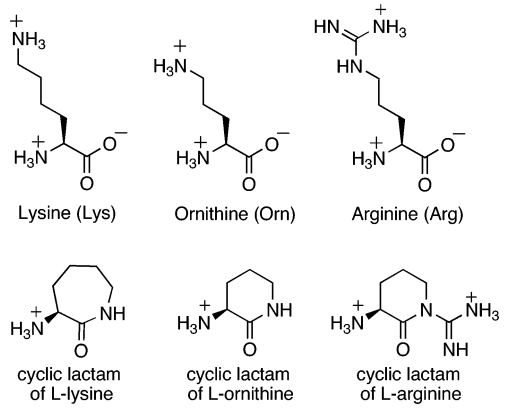

† This research was supported by SUNY at Buffalo (R.P.C.), Kapoor funds (R.P.C.), John Kapoor fellowship (P.G.), and the NYSTAR J. D. Watson Investigator Program (R.P.C.).

* To whom correspondence should be addressed. Tel: (716) 645-6800 (ext 2158). Fax: (716) 645-6963. E-mail: chengr@buffalo.edu.

[1] Abbreviations: Arg, arginine; Asp, aspartic acid; CD, circular dichroism spectroscopy; CVFF, consistent valence force field; Dab, (S)-2,4-diaminobutyric acid; Dap, (S)-2,3-diaminopropionic acid; Fmoc, 9-fluorenylmethyloxycarbonyl; Glu, glutamic acid; Gly, glycine; Lys, lysine; His, histidine; Orn, ornithine; Tyr, tyrosine.

10.1021/bi700701z CCC: $37.00
Published on Web 08/25/2007

There are several possible reasons for the utilization of Lys over Orn, including practicality of incorporation, secondary structure stability, or ion pairing energetics. For the practicality of incorporation, the putative Orn aminoacyl-tRNA may potentially self-destruct through intramolecular cyclization of the side chain amine onto the backbone ester to form a six-membered ring lactam (Chart 1), whereas the Lys aminoacyl-tRNA would not form such a lactam because of a less favorable seven-membered ring transition state and product (Chart 1). Interestingly, a similar cyclization occurs for the activated ester of protected Arg during solid-phase peptide synthesis (*24*). Nonetheless, Arg residues are effectively incorporated by the natural protein synthesis machinery. While the Arg guanidinium is more sterically hindering than the Orn ammonium, the pK_a values of both guanidinium and ammonium groups are significantly higher than physiological pH, making the nucleophilic neutral forms essentially nonexistent at pH 7. Therefore, the bioincorporation of Orn into natural proteins should be possible. For secondary structure stability, Lys exhibits a higher helix propensity than Orn (*25*, *26*). However, Lys residues are also found in non-helical secondary structures such as β-sheets or reverse turns (*27*), implying that helix propensity may not be the only reason for the utilization of Lys over Orn. As for ion-pairing interactions, Lys residues frequently participate in ion-pairing interactions in proteins (*1*, *3*), suggesting that the side chain length of Lys may affect ion-pairing energetics in protein structures.

Short α-helical peptides are convenient model systems for studying the effect of ion-pairing interactions on α-helix stability (*14*, *28*−*38*) because Glu−Lys (*i*, *i*+*4*) sequence patterns are frequently observed in natural protein α-helices (*1*, *2*). As such, interactions between positively charged residues (Lys, Orn, Arg, His) and negatively charged residues (Asp, Glu) have been studied in monomeric α-helices (*14*, *28*−*38*). These interactions have been found to be more favorable with (*i*, *i*+*4*) spacing than with (*i*, *i*+*3*) spacing (*14*, *23*, *28*−*30*). The difference between the two spacings has been attributed to the difference in the ease of making hydrogen bonds between preferred rotamer conformations (*1*). These interactions stabilize the helical conformation by up to 0.5 kcal·mol^{-1} per interaction (*23*, *28*, *32*, *35*). There has been one limited study that includes both intra-helical Glu−Lys and Glu−Orn interactions with no direct comparison between the two (*32*); therefore, the effect of Lys side chain length on these ion-pairing energetics remains to be fully understood. Herein, we report a systematic comprehensive study of the effect of side chain length on such intra-helical interactions between oppositely charged residues by circular dichroism spectroscopy and molecular mechanics calculations combined with surveys of a non-redundant protein structure database.

MATERIALS AND METHODS

Peptide Synthesis. Peptides were synthesized by solid-phase peptide synthesis using Fmoc-based chemistry (*24*, *39*). All peptides were purified by reversed-phase high performance liquid chromatography to greater than 98% purity. Concentrations were determined by UV−vis as described by Edelhoch (*40*, *41*).

Circular Dichroism Spectroscopy (CD). CD data were obtained using a 1 mm path length cell. The concentration of peptide stock solutions were determined by the tyrosine absorbance in 6 M guanidinium chloride (ϵ_{282} = 1240, ϵ_{280} = 1300, ϵ_{278} = 1390, ϵ_{276} = 1450) (*40*, *41*). CD measurements were performed at peptide concentrations close to 50 μM in 1 mM phosphate, 1 mM citrate, and 1 mM borate buffer (pH 7 in the absence and presence of 1 M NaCl and pH 2−12) at 0 °C. The data was analyzed using Kaleidagraph (Synergy Software, CA). Each reported CD value was the mean of at least three determinations. Data are expressed in terms of mean residue ellipticity (deg·cm^2·dmol^{-1}) normalized to the number of backbone amide bonds.

Calculating f_{helix} and Interaction Energy Using Modified Lifson−Roig Theory. The modified Lifson−Roig theory (*42*) that included end-capping effects (*43*) and interactions between charged residues and the helix macrodipole (*28*) was used to calculate the fraction helix (f_{helix}) of each peptide in the absence of side chain−side chain interactions (*43*). These calculations were performed using compiled computer code written in C++ on a Silicon Graphics Octane 2. Literature values for the helix propagation parameter *w* (*25*, *43*−*45*) and the N-terminal capping parameter *n* (*25*, *43*, *44*) were used for the calculations, and the helix initiation parameter υ and the C-terminal capping parameter *c* for all residues were set to 0.048 (*44*) and 1 (*44*), respectively. The contribution of interactions between charged residues and the helix macro-dipole was calculated based on the method as described by Scholtz (*28*). Modifications to the method were made to account for helical states with multiple helical segments. The fraction helix was used to calculate the predicted mean residue ellipticity at 222 nm using eq 1 (*44*).

$$\theta_{222,\text{prediction}} = f_{helix} \cdot 40{,}000 \cdot \left(1 - \frac{2.5}{N}\right) \qquad (1)$$

N is the total number of residues.

To obtain the side chain−side chain interaction energetics, the statistical weight for each specific intra-helical side chain−side chain interaction (*p*) was calculated from the experimental f_{helix} on the basis of the nesting block method (*28*, *46*). Modifications to the nesting block method were made to explicitly include helix propagation parameters for each amino acid (*25*, *43*, *44*), interactions between charged residues and helix macrodipole (*28*), and also states with multiple helical segments. For every possible state of each peptide, the f_{helix} and probability were calculated and combined. The free energy of each specific side chain−side chain interaction was calculated by ΔG = -RT·ln(*p*) (*28*),

Conformational Analysis by Molecular Mechanics. The conformational analysis was performed on a Silicon Graphics Octane 2 workstation using the Discover_3 module of the program InsightII (Accelrys, CA). The models were initially created with ideal backbone dihedral angles for α-helix with various combinations of potential low-energy side chain dihedrals. Each conformation was then minimized using the CVFF forcefield in the Discover_3 module. No cutoffs were used for the nonbonding interactions with a distance dependent dielectric constant. After minimization, each conformation was re-examined to remove duplicating conformations because minimization with different starting conformations occasionally resulted in the same final conformation. When the same conformation is represented more than once, only the lowest energy conformation is considered in further analyses.

Chart 2: Sequences for the EXaa3, EXaa4, and EXaa5 Peptides

Peptide	Sequence
EXaa3:	Ac-Tyr Gly Gly Ala (Glu Ala Ala Xaa Ala)$_3$ -NH_2
EXaa4:	Ac-Tyr Gly Gly Ala (Glu Ala Ala Ala Xaa)$_3$ Ala-NH_2
EXaa5:	Ac-Tyr Gly Gly (Glu Ala Ala Ala Ala Xaa)$_3$ -NH_2

Xaa: Lys, Orn, Dab, Dap

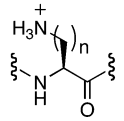

n = 1, Dap, *S*-2,3-diaminopropionic acid
2, Dab, *S*-2,4-diaminobutyric acid
3, Orn, L-ornithine
4, Lys, L-lysine

Survey of Glu−Lys (i, i+3) and (i, i+4) Salt Bridges in Protein α*-Helices.* The survey was performed on PDBselect (Dec 2003, 25% threshold) (*47*), a database of non-redundant protein chains. The α-helical conformation for each residue was defined by hydrogen bonding as described by Kabsch and Sander (*48*). Segments of six or more α-helical residues were considered to avoid end effects. The occurrence was compiled for Glu−Lys (*i, i+3*) and (*i, i+4*) residue patterns. The propensity of each residue pattern was calculated by dividing the occurrence of the sequence pattern in α-helices by the expected occurrence for the sequence pattern based on the random protein structures in PDBselect. The expected occurrence and the corresponding standard deviation were obtained by bootstrapping (*49*) the sequence pattern across the PDBselect database. Dividing the difference between the occurrence and the expected occurrence by the standard deviation gave the *z* value, which was used to obtain the *P* value based on a normal distribution (*50*, *51*). Each individual occurrence was then visually inspected for the presence of a Glu−Lys salt bridge using the program InsightII (Accelrys, CA) on an Silicon Graphics Octane 2 workstation. A salt bridge was considered to be present if any of the oxygens of the side chain carboxylate of Glu was within 3 Å of the nitrogen of the side chain amine of Lys.

RESULTS

Design and Synthesis of Monomeric α*-Helical Peptides.* The peptides were designed based on monomeric α-helical peptides containing potential Glu−Lys (*i, i+3*) or (*i, i+4*) interactions as described by Baldwin and co-workers (*14*). Glutamate was chosen as the negatively charged amino acid because Glu−Lys (*i, i+4*) sequence patterns are frequently observed in natural protein α-helices (*1*, *2*). The peptides are named according to the three-letter code of the positively charged residue (Xaa = Lys, Orn, Dab, and Dap) and the spacing between Glu and the downstream Xaa (Chart 2). Since an ideal α-helix would have 3.6 residues per turn, the EXaa3 and EXaa4 peptides could potentially have interactions between oppositely charged residues spaced 3 and 4 residues apart, respectively (Chart 2). The Exaa5 peptides have oppositely charged resides spaced 5 residues apart (Chart 2), which should not interact, on the basis of the α-helix geometry and as shown by Scholtz and co-workers (*30*). While the negatively charged residue Glu was incorporated in all of the peptides, the positively charged residue Xaa was systematically shortened from Lys (4 methylenes) to (*S*)-2,3-diaminopropionic acid (Dap, 1 methylene) (Chart 2). The overall distribution of the charged residues was designed to stabilize the α-helix macrodipole by placing Glu closer to the N-terminus than the positively charged residue Xaa (*14*). Tyr was incorporated to facilitate concentration determination by UV−vis, and the Gly−Gly intervening sequence was included to minimize interference in the CD signal by the Tyr chromophore (*52*).

The peptides were synthesized by solid-phase peptide synthesis using Fmoc-based chemistry (*24*, *39*). All peptides were purified by reversed-phase high performance liquid chromatography to greater than 98% purity. The peptide concentrations were determined by UV−vis as described by Edelhoch (*40*, *41*). Size-exclusion chromatography results were consistent with monomers for all peptides except peptides EDap3 and EDap4, both of which exhibited apparent molecular weights larger than monomers, most likely due to the lack of folding as shown by circular dichroism spectroscopy (*vide infra*). Furthermore, sedimentation equilibrium data were consistent with monomers for all peptides except peptide EDap4, which showed a hint of larger order aggregation. Therefore, intermolecular interactions are most likely not contributing to the helical content observed by circular dichroism spectroscopy (CD).

Circular Dichroism Spectroscopy. The circular dichroism (CD) spectra of the peptides were obtained at pH 7 in the absence of NaCl (Figure 1). The CD spectra of ELys3, ELys4, and EOrn4 are similar to the CD spectra of analogous peptides reported by Baldwin (*14*) and Stellwagen (*32*). The magnitude of the CD signal at 222 nm reflects the α-helical content of a peptide (*53*). On the basis of CD spectra, the helical content of EXaa5 peptides follows the trend ELys5 > EOrn5 > EDab5 > EDap5 (Figure 1A). This trend is consistent with the helix propensity of the positively charged residue Xaa: Lys > Orn > Dab > Dap (*25*). In contrast, the helical content of EXaa4 peptides follows the trend: ELys4 ∼ EOrn4 ∼ EDab4 ≫ EDap4 (Figure 1B). Peptides ELys4, EOrn4, and EDab4 exhibit significant helicity, whereas EDap4 shows diminished helical content. Apparently, the Lys side chain can be shortened by two methylenes without affecting the helical content of the EXaa4 peptides, suggesting significant Glu−Xaa (*i, i+4*) interactions involving Lys, Orn, and Dab. Interestingly, the helical content of EXaa3 peptides follows the trend ELys3 ≫ EOrn3 > EDab3 > EDap3 (Figure 1C). Only peptide ELys3 is significantly helical, whereas the other three EXaa3 peptides are relatively non-helical. On the basis of these results, it appears that only the Lys side chain has sufficient length to support any Glu−Xaa (*i, i+3*) interaction.

The CD signal at 222 nm for all peptides were measured between pH 2 and 12 (Figure 2) to provide insight into the nature of the Glu−Xaa intra-helical interactions. However, the high pH data could not be interpreted without ambiguity because the Tyr phenol side chain has a pK_a near 10, and aromatic groups may contribute to the CD signal (*52*). Since the helix dipole can perturb the pK_a by 1.6 pH units (*54*, *55*), the discussion will focus on data between pH 2 and 7. In this pH range, all EXaa5 peptides have similar CD signals. In contrast, the magnitude of the CD signal is weaker at pH 2 compared to pH 7 for all EXaa4 peptides except ELys4, which exhibited minimal pH dependence in its CD signal. Interestingly, there is minimal change in CD signal for the EXaa3 peptides.

The CD spectra of the EXaa3, EXaa4, and EXaa5 peptides at pH 2 were acquired to probe the intra-helical Glu−Xaa interactions involving neutral Glu^0 side chains (Figure 3).

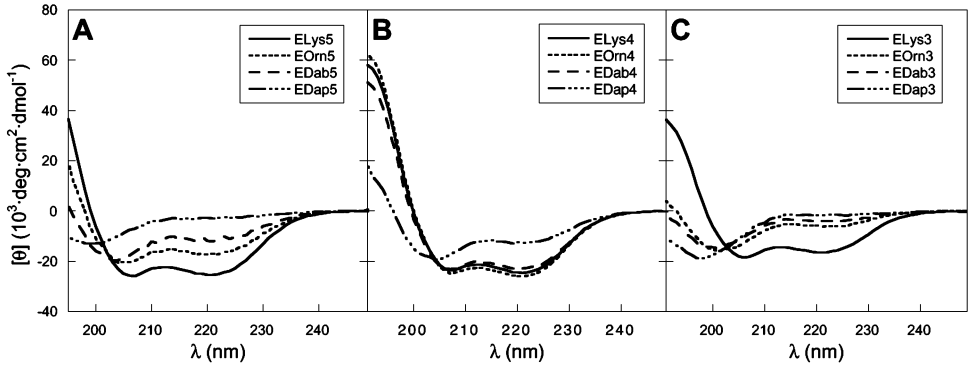

FIGURE 1: Circular dichroism spectra of the peptides at pH 7 (273 K) in 1 mM phosphate, borate, and citrate buffer in mean residue ellipticity (panel A, ELys5, EOrn5, EDab5, and EDap5; panel B, ELys4, EOrn4, EDab4, and EDap4; panel C, ELys3, EOrn3, EDab3, and EDap3).

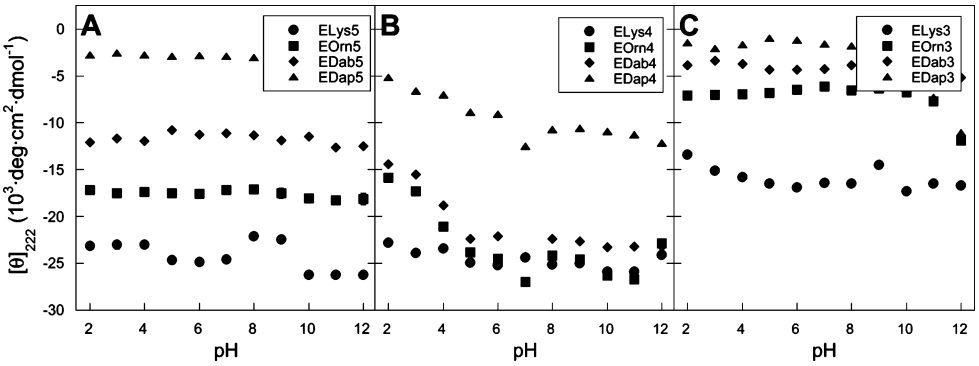

FIGURE 2: Circular dichroism signal at 222 nm of the peptides at pH 2−12 (273 K) in 1 mM phosphate, borate, and citrate buffer in mean residue ellipticity (panel A, ELys5, EOrn5, EDab5, and EDap5; panel B, ELys4, EOrn4, EDab4, and EDap4; panel C, ELys3, EOrn3, EDab3, and EDap3).

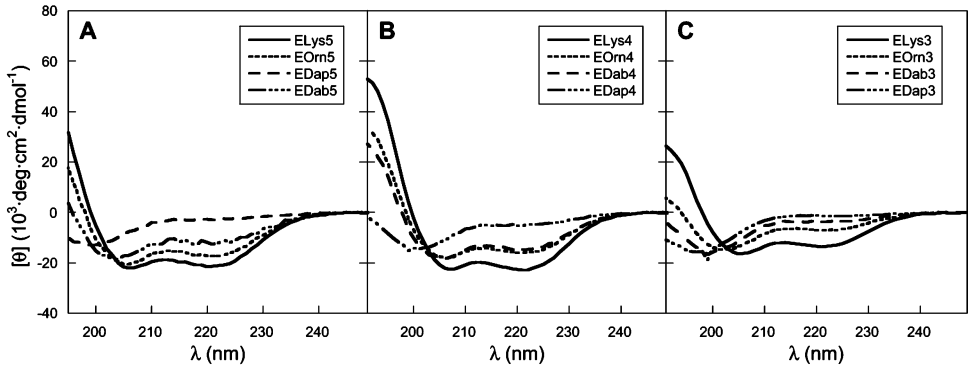

FIGURE 3: Circular dichroism spectra of the peptides at pH 2 (273 K) in 1 mM phosphate, borate, and citrate buffer in mean residue ellipticity (panel A, ELys5, EOrn5, EDab5, and EDap5; panel B, ELys4, EOrn4, EDab4, and EDap4; panel C, ELys3, EOrn3, EDab3, and EDap3).

Similar to the CD results at pH 7, the trend for the helical content of the EXaa5 peptides is consistent with the helix propensity of the positively charged residue Xaa (Figure 3A). At pH 2, the helical content for the EXaa4 peptides follows the trend ELys4 > EOrn4 ∼ EDab4 > EDap4 (Figure 3B). This result suggests that the side chain length of Lys plays a significant role for Glu^0−Lys (*i*, *i*+*4*) interactions at pH 2, for which Glu is most likely neutral. This is in sharp contrast to the results at pH 7, for which the side chain length does not appear to be critical for Glu^-−Lys (*i*, *i*+*4*) interactions. Similar to the CD results at pH 7, the helical content at pH 2 for the EXaa3 peptides follows the trend ELys3 ≫ EOrn3 > EDab3 > EDap3 (Figure 3C).

Calculating the Intra-Helical Glu−Xaa Interaction Energetics at pH 7 and 2. The side chain−side chain interaction energy ($\Delta G_{pH\ 7\ interaction}$ and $\Delta G_{pH\ 2\ interaction}$) between oppositely charged residues were calculated using the nesting block method (*28*, *46*) based on the modified Lifson−Roig theory (*28*, *42*−*44*), accounting for the charged side chain−helix dipole interactions for all states and increased Glu helix propensity upon protonation (Table 1). At pH 7, the Glu^-−Lys (*i*, *i*+*4*) interaction is more favorable compared to the Glu^-−Lys (*i*, *i*+*3*) interaction, and the energies are similar to values reported by other researchers (*23*, *28*, *30*). For peptides ELys5 and EOrn5, essentially no Glu^-−Xaa (*i*, *i*+*5*) interaction is observed, consistent with the α-helical structure. Interestingly, peptides EDab5 and EDap5 exhibit less helical character compared to the expected values without any intra-helical side chain−side chain interactions. This result suggests that Dab−Glu^- and Dap−Glu^- (*i*, *i*+*1*) interactions may be stabilizing non-helical conformations; analogous helix destabilizing interactions have been reported by Scholtz

Table 1: Energetics[a] of Intrahelical Interactions between Glu and Xaa at pH 7 and 2

residue *i*	residue *i* + *n*	*n*	$\Delta G_{\text{pH 7 interaction}}$ (cal·mol^{-1})	$\Delta G_{\text{pH 2 interaction}}$ (cal·mol^{-1})	$\Delta\Delta G^{d}$ (cal·mol^{-1})
Glu	Lys	5	−84.7 ± 51.4	−21.2 ± 15.6	−63.7 ± 53.1
Glu	Orn	5	0[b]	0[b]	
Glu	Dab	5	ND[c]	ND[c]	
Glu	Dap	5	ND[c]	ND[c]	
Glu	Lys	4	−459 ± 34	194 ± 31	−265 ± 46
Glu	Orn	4	−742 ± 43	125 ± 34	−617 ± 53
Glu	Dab	4	−837 ± 36	281 ± 38	−556 ± 52
Glu	Dap	4	−781 ± 43	0[b]	−781 ± 43
Glu	Lys	3	−256 ± 36	−143 ± 32	−113 ± 48
Glu	Orn	3	0[b]	ND[c]	
Glu	Dab	3	0[b]	ND[c]	
Glu	Dap	3	0[b]	ND[c]	

[a] The energetic values $\Delta G_{\text{pH 7 interaction}}$ and $\Delta G_{\text{pH 2 interaction}}$ were calculated on the basis of the nesting block method (*28*, *46*). [b] The experimental results are within error of theoretically calculated values without any side chain−side chain interaction. [c] Not determined because the experimental results exhibit lower helical content compared to the theoretically calculated values without any side chain−side chain interaction (see main text for reason). [d] $\Delta\Delta G = \Delta G_{\text{pH 7 interaction}} - \Delta G_{\text{pH 2 interaction}}$.The difference in side chain−side chain interaction energy at pH 7 and 2 reflects the contribution of electrostatics in the Glu−Xaa interaction.

and co-workers (*28*). More importantly, the Glu^{-}−Xaa (*i*, *i*+*4*) interaction energy follows the trend Lys < Orn < Dab ∼ Dap. For EXaa3 peptides, only ELys3 exhibits any favorable Glu^{-}−Xaa (*i*, *i*+*3*) interaction energy.

The Glu^{0}−Xaa interactions (involving the protonated neutral Glu^{0}) would represent the nonelectrostatic components of the Glu^{-}−Xaa interaction. The side chain−side chain interaction energies at pH 2 ($\Delta G_{\text{pH 2 interaction}}$) represent the upper limit for interactions involving Glu^{0} because the CD signals were not unambiguously leveled off with decreasing pH at pH 2. Therefore, there may be some residual electrostatic interactions involving formally charged Glu^{-}. Similar to the results at pH 7, the EXaa5 peptides do not exhibit any significant Glu^{0}−Xaa (*i*, *i*+*5*) interaction at pH 2, consistent with the α-helical structure. At pH 2, all EXaa4 peptides exhibit varying degrees of Glu^{0}−Xaa (*i*, *i*+*4*) interaction except for EDap4 (Table 1). These results suggest that the Glu^{-}−Dap (*i*, *i*+*4*) interaction at pH 7 completely relies on the formal negative charge on Glu^{-}, whereas the longer side chains are not as dependent on the negative charge on Glu^{-}. For EXaa3 peptides, only ELys3 exhibits any Glu−Xaa (*i*, *i*+*3*) interaction energy at pH 2.

The Lys side chain length does not appear to be critical for supporting the helix for EXaa4 peptides on the basis of the CD data at pH 7 (Figure 1B). However, the Lys side chain length is extremely important for supporting the helix for EXaa3 peptides (Figure 1C). The simple explanation would be that side chain lengths 2 methylenes shorter than Lys remain capable of reaching to interact with Glu for a Glu−Xaa (*i*, *i*+*4*) interaction. Similarly, only Lys has a side chain long enough to interact with Glu for a Glu−Xaa (*i*, *i*+*3*) interaction. It seems that sufficient side chain length to reach the upstream Glu for the two different spacings is the major issue. However, the interaction energetics at pH 7 based on the same CD data apparently contradicts this simple explanation. The Glu−Xaa (*i*, *i*+*4*) interaction energy increases with decreasing side-chain length, whereas the Glu−Xaa (*i*, *i*+*3*) interaction is practically nonexistent for

Chart 3: (Panel A) Sequence for the MEXaa3 and MEXaa4 Peptides used in the Conformational Analysis by Molecular Mechanics Calculations. (Panel B) Newman Projections of the Three Low Energy χ_1 Dihedrals gauche−, trans, and gauche+. (Panel C) Three-dimensional Model of a Generic Pentapeptide with the Three Low Energy χ_1 Dihedrals for Residues *i*, *i*+*3*, and *i*+*4* Highlighted[a]

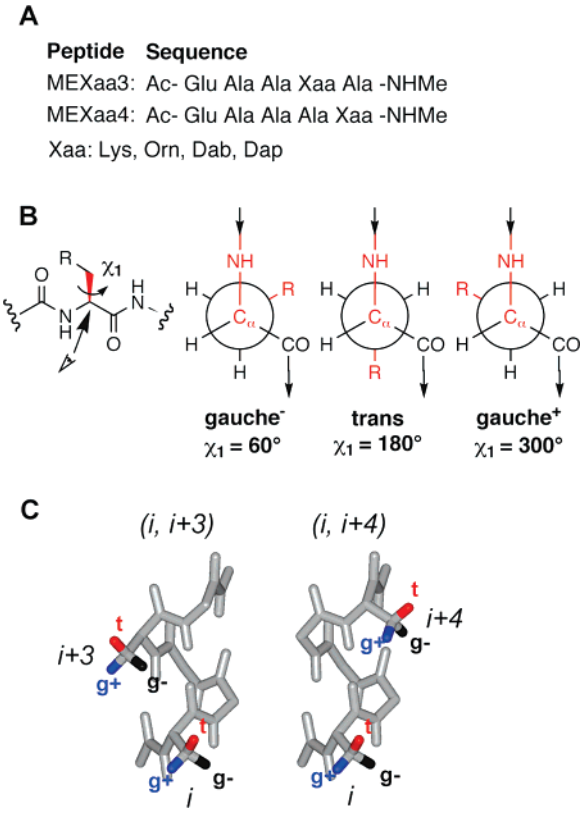

[a] The two more stable χ_1 conformations *trans* and *gauche*+ are red and blue, respectively. The less stable χ_1 conformation *gauche*− is black.

residues shorter than Lys. To resolve this apparent contradiction, conformational analysis on relevant model peptides was performed.

Conformational Analysis of Short Model Peptides. A detailed conformational analysis on short model peptides was performed by molecular mechanics calculations. Two series of peptides were investigated: MEXaa3 and MEXaa4 (Chart 3A). All peptides included one potential side chain−side chain interaction between Glu^{-} and a positively charged residue (Lys, Orn, Dab, or Dap) either three or four residues apart. For each χ angle, three possible low-energy staggered conformations were considered: gauche- (60°, *g*−), trans (180°, *t*), and gauche+ (300°, *g*+) (Chart 3B) (*56*, *57*). For the χ_1 dihedral of a residue in an α-helix in nature, the *t* and *g*+ conformations are known to be more prevalent and more stable than the *g*− conformation (*56*, *57*) because of significant gauche interactions in the *g*− conformation and steric clashes with the nearby backbone. Regardless, all possible χ angle combinations for Glu and the positively charged residue Xaa were investigated. A combined total of 12,960 conformations were minimized with no restraints.

All conformations remained helical upon minimization. The interaction between oppositely charged residues with (*i*, *i*+*3*) and (*i*, *i*+*4*) spacings can be compared by evaluating the energies of the lowest energy conformers for the MEXaa3

Table 2: Summary of Low Energy Conformations from Conformational Analysis of MEXaaN Peptides by Molecular Mechanics Calculations

	lowest energy conformer	conformations within 5 kcal of the lowest energy conformer		
peptide	energy (kcal)	no.[a]	salt bridge[b] (%)	major conformations number(Glu χ_1, Xaa χ_1)[c]
MEDap3	37.9	5	0%	4(*t*, *g*−)
MEDab3	36.4	14	64%	9(*t*, *g*−), 4(*g*+, *g*−)
MEOrn3	37.5	20	70%	8(*t*, *g*−), 7(*g*+, *g*−),
MELys3	41.4	33	73%	13(*t*, *t*), 9(*g*+, *g*+)
MEDap4	34.9	3	33%	3(*t*, *g*+)
MEDab4	29.8	4	100%	4(*t*, *g*+)
MEOrn4	30.2	6	83%	6(*t*, *g*+)
MELys4	40.1	21	86%	9(*t*, *g*+), 6(*g*−, *g*+)

[a] The number of conformations within 5 kcal of the lowest energy conformer for each peptide. [b] The percentage of conformations within 5 kcal of the lowest energy conformer with a Glu−Xaa salt bridge, which is a hydrogen-bonded ion pair.

and MEXaa4 peptides (Table 2). Peptides with the same positively charged residue (eg., MELys3 and MELys4) can be compared because the peptides were designed to have the same constituting atoms represented by the same force-field parameters. For peptides MELys3 and MELys4, there is a small difference between the lowest energy conformations, suggesting that the Glu−Lys interaction is energetically similar for the two different spacings. For all the other MEXaa peptides, the MEXaa4 peptides are significantly lower in energy than the corresponding MEXaa3 peptides, suggesting that Glu−Xaa (Xaa = Orn, Dab, and Dap) interaction is energetically more favorable for the (*i*, *i*+*4*) than the (*i*, *i*+*3*) spacing. Furthermore, a larger energy difference between the two spacings was observed for peptides involving Orn and Dab compared to that for peptides involving Dap. These results are consistent with the earlier CD experiments (Figure 1) and interaction energies ($\Delta G_{\text{pH 7 interaction}}$, Table 1).

Conformations within 5 kcal of the lowest energy conformer for each peptide were then examined in detail (Table 2) because room temperature can provide up to 5 kcal·mol^{-1} of thermal energy. There are more conformations for the MEXaa3 peptides compared to the corresponding MEXaa4 peptides. Furthermore, the MEXaa4 peptides exhibit a higher percentage of conformations with intra-helical salt bridges as compared to the corresponding MEXaa3 peptides, consistent with the CD data at pH 7 (Figure 1).

The combination of χ_1 dihedrals is represented in parentheses, designating the conformation for residue *i* followed by that for *i*+*3* or *i*+*4*. For example, the conformation with *t* for both residues *i* and *i*+*3* would be designated (*t*, *t*) for (*i*, *i*+*3*). The χ_1 dihedral combination for the MEXaa3 low energy conformers is either (*t*, *g*−) or (*g*+, *g*−), when Xaa is not Lys (Table 2 and Figure 4). These conformations involve the high energy χ_1 dihedral *g*− for the positively charged Xaa residue. Interestingly, this high energy χ_1 dihedral seems to be necessary for projecting the Xaa side chain toward the upstream Glu to promote Glu−Xaa (*i*, *i*+*3*) interactions (Chart 3C). In contrast, the lower energy conformers of MELys3 involve the (*i*, *i*+*3*) χ_1 dihedral combinations (*t*, *t*) and (*g*+, *g*+), both of which exhibit lower energy χ_1 dihedrals for the *i*+*3* residue than *g*−. On the basis of these results, the apparent absence of stabilizing (*i*, *i*+*3*) interactions in the EXaa3 peptides (except ELys3) as seen from CD can be attributed to the need to populate a high energy χ_1 dihedral to accommodate the salt bridge, not the lack of sufficient side chain length to form the salt bridge. Importantly, the side chain length enables Lys to simultaneously adopt a low energy χ_1 dihedral and form a salt bridge. This highlights the uniqueness of Lys compared to the shorter amino acids and the conformational origin of the effect of the side chain length on intra-helical ion-pairing interactions.

For the χ_1 dihedrals of all MEXaa4 peptides, the (*t*, *g*+) combination is the most prevalant (Table 2 and Figure 4), with increasing variation as the side chain length increases. This (*t*, *g*+) χ_1 dihedral combination is ideal for promoting intra-helical side chain−side chain interaction without the higher energy *g*− conformation (Chart 3C). These results would explain the higher helical content for the EXaa4 peptides compared to the corresponding EXaa3 peptides (Figure 1). Furthermore, the decrease in interaction energy with increasing side chian length is most likely due to higher entropy penalty. Although these molecular mechanics calculation results seem to explain the experimental data, it remained unclear whether or not these conformational preferences are observed in natural proteins. To further confirm the results from this conformational analysis, intra-helical Glu−Lys salt bridges in natural proteins were examined for comparison.

Intra-Helical Glu−Lys Salt Bridges in Protein Structures. A survey was performed on the non-redundant protein structure database PDBselect (Dec 2003, 25% threshold) in order to study the side chain conformations that support intra-helical side chain−side chain interactions in naturally occurring proteins (*47*). The α-helical conformation was defined by hydrogen bonding as described by Kabsch and Sander (*48*). Only α-helices of 6 residues or longer were considered, excluding α-helices with less than one turn. The number of occurrences of Glu−Lys (*i*, *i*+*3*) and (*i*, *i*+*4*) sequence patterns were 808 and 784, respectively. The propensity for the Glu−Lys (*i*, *i*+*3*) and (*i*, *i*+*4*) sequence patterns were 2.48 ± 0.14 and 2.11 ± 0.11, respectively, indicating that both sequence patterns occur more than twice the expected occurrence based on all protein structures. Both Glu−Lys sequence patterns had *P* values of less than 10^{-5}, indicating that the occurrence of these patterns in α-helices were significantly different from the expected occurrence based on all protein structures, similar to published results by Scheraga and co-workers (*2*). The three-dimensional structures of these occurrences were then examined in detail. Using 3 Å as the N−O cutoff distance for a Glu−Lys salt bridge, there were 43 and 24 salt bridges for (*i*, *i*+*3*) and (*i*, *i*+*4*) spacings, respectively. Only a small number of the sequence patterns were manifested as salt bridge interactions in the protein structure, similar to findings by Thornton and co-workers (*3*). Furthermore, these salt bridges were predominantly on the surface of the proteins and were solvent exposed. In general, the combinations of χ_1 dihedrals for the Glu−Lys intra-helical salt bridges in natural protein structures were similar to those from the molecular mechanics calculations (Figure 4, last two columns), validating the conformational origin of the uniqueness of Lys in intra-helical ion-pairing interactions.

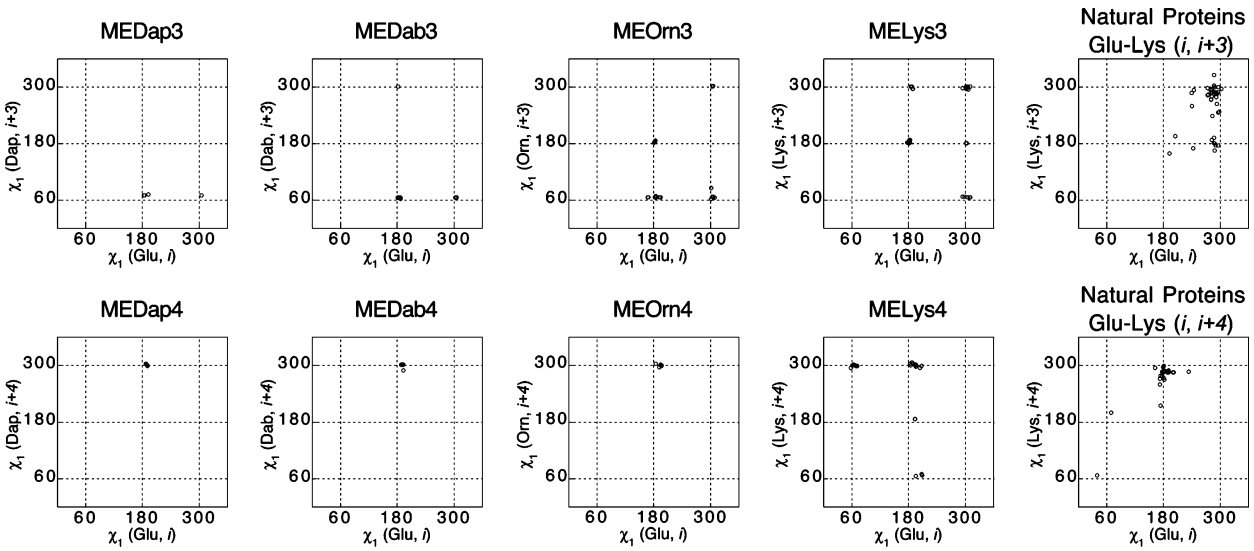

FIGURE 4: χ_1(Glu, *i*)-χ_1(Xaa, *i*+*3* or *i*+*4*) plots for the MEXaa3 peptides (first four plots in top row) and MExaa4 peptides (first four plots in bottom row) within 5 kcal of lowest energy conformation from the conformational analysis by molecular mechanics calculation are in the first four columns (top row from left to right, MEDap3, MEDab3, MEOrn3, and MELys3; bottom row from left to right, MEDap4, MEDab4, MEOrn4, and MELys4). The side chain conformation of intra-helical Glu−Lys (*i*, *i*+*3*) and Glu−Lys (*i*, *i*+*4*) salt bridges from the survey of natural proteins are in the last column. For the three low energy χ_1 dihedrals, gauche ($\chi_1 = 60°$) is higher in energy than trans ($\chi_1 = 180°$) and gauche+ ($\chi_1 = 300°$).

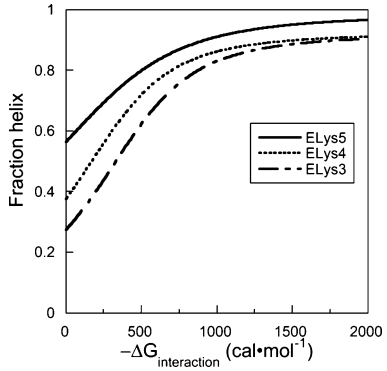

FIGURE 5: Expected fraction helix of the peptides ELys5, ELys4, and ELys3 plotted as a function of the negative of the putative interaction energy ($-\Delta G_{interaction}$, cal•mol^{-1}).

DISCUSSION

Direct comparisons between the CD spectra of peptides with different spacings are not indicative of the difference in interaction energetics. In particular, the sequence of ELys5 inherently favors the helical conformation compared to ELys4 and ELys3 (with no intrahelical interactions) because of the total number of Ala residues and the longer stretches of Ala for the ELys5 (Figure 5). Furthermore, the helical content would be lower for ELys3 compared to ELys4 given the same Glu−Lys interaction energy (Figure 5). Therefore, direct comparisons between the CD spectra from different peptide series cannot be used to even qualitatively compare the Glu−Lys (*i*, *i*+*3*), (*i*, *i*+*4*), and (*i*, *i*+*5*) interaction energies. This is because the observed helical content is the manifestation of both helix-stabilizing side chain side-chain interactions and the inherent features of the sequences, as previously deduced by Baldwin (*29*). Obtaining intra-helical interaction energetics quantitatively requires calculations using the modified Lifson−Roig theory based on the CD data. Results based on this analysis show that the side chain length of Lys is critical for the existence of the Glu$^-$−Xaa (*i*, *i*+*3*) interaction, whereas the Glu$^-$−Xaa (*i*, *i*+*4*) interaction energetics increases with decreasing side chain length (Table 1).

The calculations based on the Lifson−Roig theory used parameters reported by Baldwin and co-workers (*25*, *43*, *44*). The parameters were derived from 58 different Ala-based peptides with 16−20 residues, 3 or 4 Lys (or Gln) residues, and 2.33−4.00 Ala residues for every Lys (or Gln) residue (*44*). These sequence characteristics are similar to the peptides studied in this article. Since the Baldwin parameters are derived from peptides with these sequence characteristics, they are particularly suitable for analyzing these peptides. However, these same parameters may not be suitable for peptides that differ significantly from these sequences, as shown by Kemp (*26*, *58*). Nonetheless, peptides with analogous length and similar sequence characteristics can be analyzed using these parameters derived by Baldwin (*25*, *43*, *44*).

Intra-helical Glu−Lys (*i*, *i*+*3*) and (*i*, *i*+*4*) interactions have been attributed to electrostatics (*14*, *28*, *29*), hydrogen bonding (*14*, *29*), and possibly hydrophobics (*59*). Electrostatic interactions occur between two formally charged species. Salt bridges occur when the two oppositely charged functionalities are also hydrogen bonded (*14*, *15*). However, a hydrogen bond between a formal charge and a neutral functionality is considered to be a hydrogen bond (*15*, *60*) that is typically stronger than hydrogen bonds between two neutral species. To gain insight into how the side chain length affects the contributing factors, we made comparisons between the Glu−Xaa interactions at pH 7 and 2. Changing the pH from 7 to 2 should protonate and neutralize the carboxylate side chain of the negatively charged residue Glu$^-$. This would disrupt the electrostatic interactions with the negatively charged Glu$^-$ (including Glu$^-$−Xaa and Glu$^-$-helix macrodipole) and would also increase the helix propensity of Glu (*28*). Thus, changes in CD signal should reflect changes in both electrostatic interactions and helix propensity. The lack of significant change in the CD signal for the Exaa5 and EXaa3 peptides suggests that these effects

most likely cancel one another (Figure 2A and C). More specifically, the loss of favorable electrostatic interaction between Glu^- and the helix macrodipole is compensated by the increase in Glu helix propensity upon protonation of the Glu^- side chain. Furthermore, there is a slight hint of a stronger CD signal at pH 7 compared to pH 2 for ELys3 (Figure 2C), reflecting the extra loss of the weak Glu^-−Lys (*i, i+3*) electrostatic interaction upon neutralization of Glu. Similarly, the loss of Glu^-−Xaa (*i, i+4*) interaction is clearly visible for all EXaa4 peptide except ELys4 (Figure 2B), which appears to be indifferent to the neutralization of Glu^-. Clearly, the pH independent behavior is unique for Lys compared to the Lys analogues with shorter side chain length. The Glu^0−Lys (*i, i+4*) interaction energy remains more favorable than the Glu^0−Lys (*i, i+3*) interaction energy at pH 2 (Table 1), similar to the values reported by other researchers (*30*). The difference between side chain−side chain interaction energy at pH 7 and 2 represents the lower limit of the contribution of electrostatics to the Glu^-−Xaa interaction ($\Delta\Delta G$, Table 1) because of the apparent incomplete neutralization of the Glu^- side chain at pH 2. Accordingly, the Glu^-−Lys (*i, i+3*) interaction is predominantly electrostatic on the basis of the $\Delta\Delta G$. Among Glu^-−Xaa (*i, i+4*) interactions at pH 7, the electrostatic contribution to the interaction energy followed the trend Dap ≫ Orn > Dab > Lys. The lack of any Glu^0−Dap (*i, i+4*) interaction at pH 2 suggests that the interaction at pH 7 is purely electrostatics. Furthermore, significant attenuation of the Glu^-−Xaa (*i, i+4*) interaction for Dab and Orn upon protonating Glu^- at pH 2 implies that electrostatics plays a significant role in these interactions at pH 7. Importantly, the Glu^-−Lys (*i, i+4*) interaction was the least affected by pH compared to that in Lys analogues with shorter side chains. This may be due to significant side chain−side chain hydrogen bonding (*14*, *29*) and hydrophobic interaction (*59*). More specifically, the residual side chain−side chain hydrogen bond would serve to bring the two terminal functionalities together, whereas the hydrophobic methylenes on the Lys side chain would serve to shield the helix hydrogen bond and stabilize the helix (*26*, *61*, *62*). These results suggest that the side chain length is critical for Lys to support significant Glu−Xaa (*i, i+4*) interactions at different pH values because of the relatively low contribution of the electrostatic component to the interaction.

Molecular mechanics calculations show that the combinations of χ_1 dihedrals facilitate the projection of the interacting side chains toward one another to promote intra-helical interactions (*vide supra*), even if unfavorable $\chi 1$ dihedrals are necessary. However, the combination of χ_1 dihedrals deviates from the simple predictions for longer side-chain lengths because the lengthy side chains are capable of redirecting the side chain functionality. This is best exemplified by Lys, which is capable of populating more favorable dihedrals and yet still supporting an intra-helical Glu−Lys (*i, i+3*) interaction. Regardless of spacing, Lys appears to be unique in its conformational properties in intra-helical side chain−side chain interactions compared to the Lys analogues with shorter side chain lengths. Furthermore, a number of these low energy conformations in the molecular mechanics calculation were also observed in a survey of intra-helical Glu−Lys salt bridges in natural protein structures (Figure 4).

The combination of the high Lys helix propensity and small electrostatic component in the Glu−Lys (*i, i+4*) interaction supports the high fraction helix for peptide ELys4 under various conditions, showing the importance of the Lys side chain length to support the high fraction helix for monomeric α-helices with intra-helical ion pairing. However, a study on a tetrameric coiled-coil system indicated that inter-helical ion-pairing was not significantly affected by shortening the side chain length from Lys to Orn (*63*). Furthermore, there have been a handful of studies on stabilizing effects of Lys containing inter-strand ion pairs in β-sheet systems (*64*−*68*). It is most likely that the conformational preferences for Lys revealed in this article will not be transferable to β-sheets; however, the nonelectrostatic components (hydrogen bonding and hydrophobics) for Glu−Lys ion-pairing interaction should remain significant in non-helical structures. Regardless, the effect of the Lys side chain length in β-sheet systems remains to be fully explored. Interestingly, β-hLys and β-hOrn have been used interchangeably in ion-pairing interactions to stabilize β-peptide 14-helices (*69*−*71*). The role of the Lys side chain length in stabilizing helical conformations in such non-natural oligomers also remains to be fully investigated.

CONCLUSIONS

CD experiments at pH 7 show that Lys is the only residue capable of supporting a helix-stabilizing Glu−Xaa (*i, i+3*) interaction, but Lys, Orn, Dab, and Dap are all capable of supporting a helix-stabilizing Glu−Xaa (*i, i+4*) interaction. Furthermore, the helical content of the peptide with Glu−Lys (*i, i+4*) interactions did not alter significantly upon lowering the pH based on CD data. However, shortening the Lys side chain by only one methylene (Orn) results in marked decrease in helical content upon lowering the pH from 7 to 2. In addition, the electrostatic component of the Glu−Xaa (*i, i+4*) interaction increases significantly upon shortening the Lys side chain by one methylene to Orn. On the basis of molecular modeling studies, Lys is the only residue with sufficient length to simultaneously populate a low energy χ_1 dihedral and promote a Glu−Xaa (*i, i+3*) interaction, whereas Orn, Dab, and Dap side chains are too short to interact with Glu without populating an unfavorable χ_1 dihedral. In contrast, Glu−Xaa (*i, i+4*) interactions inherently involve low energy χ_1 dihedrals. Furthermore, the combinations of χ_1 dihedrals for Glu−Lys (*i, i+3*) and (*i, i+4*) intra-helical salt bridges in natural protein structures are observed in the molecular mechanics calculations. These results highlight the drastic effect of the Lys side chain length on side chain−side chain interactions. The underlying reason for the exceptional ion-pairing characteristics of Lys is likely a combination of conformational preference, electrostatics, hydrogen bonding, and hydrophobics. Interestingly, nature may have chosen Lys to form robust interactions with negatively charged functional groups for enhanced stability. Nonetheless, residues with shorter side chains such as Orn or Dab may be useful for designing conformation-dependent pH sensitive switches (*72*−*77*) or sensors (*78*, *79*).

ACKNOWLEDGMENT

We thank Robert Fairman and Bashkim Kokona for sedimentation equilibrium experiments, Donald Gullickson

for help with the theoretical calculation of helical content, Hsien-Po Chiu and Marc J. Koyack for help with synthesizing four of the peptides, Donald Engel for help on the survey, Teng-Kai (George) Yang for help with bootstrapping, and Cheu-Pyeng Cheng for helpful discussions.

SUPPORTING INFORMATION AVAILABLE

Experimental details of the synthesis and characterization of the peptides. This material is available free of charge via the Internet at http://pubs.acs.org.

REFERENCES

1. Klingler, T. M., and Brutlag, D. L. (1994) Discovering structural correlations in α-helices, *Protein Sci. 3*, 1847−1857.
2. Maxfield, F. R., and Scheraga, H. A. (1975) Effect of neighboring charges on helix forming ability of charged amino-acids in proteins, *Macromolecules 8*, 491−493.
3. Barlow, D. J., and Thornton, J. M. (1983) Ion-pairs in proteins, *J. Mol. Biol. 168*, 867−885.
4. Dill, K. A. (1990) Dominant forces in protein folding, *Biochemistry 29*, 7133−7155.
5. Makhatadze, G. I., and Privalov, P. L. (1995) Energetics of protein structure, *Adv. Protein Chem. 47*, 307−425.
6. Pace, C. N. (2000) Single surface stabilizer, *Nat. Struct. Biol. 7*, 345−346.
7. Elcock, A. H., and McCammon, J. A. (1997) Continuum solvation model for studying protein hydration thermodynamics at high temperatures, *J. Phys. Chem. B 101*, 9624−9634.
8. Elcock, A. H. (1998) The stability of salt bridges at high temperatures: implications for hyperthermophilic proteins, *J. Mol. Biol. 284*, 489−502.
9. Malakauskas, S. M., and Mayo, S. L. (1998) Design, structure and stability of a hyperthermophilic protein variant, *Nat. Struct. Biol. 5*, 470−475.
10. Matthews, B. W., Weaver, L. H., and Kester, W. R. (1974) Conformation of thermolysin, *J. Biol. Chem. 249*, 8030−8044.
11. Thomas, A. S., and Elcock, A. H. (2004) Molecular simulations suggest protein salt bridges are uniquely suited to life at high temperatures, *J. Am. Chem. Soc. 126*, 2208−2214.
12. Xiao, L., and Honig, B. (1999) Electrostatic contributions to the stability of hyperthermophilic proteins, *J. Mol. Biol. 289*, 1435−1444.
13. Yip, K. S. P., Britton, K. L., Stillman, T. J., Lebbink, J., De Vos, W. M., Robb, F. T., Vetriani, C., Maeder, D., and Rice, D. W. (1998) Insights into the molecular basis of thermal stability from the analysis of ion-pair networks in the glutamate dehydrogenase family, *Eur. J. Biochem. 255*, 336−346.
14. Marqusee, S., and Baldwin, R. L. (1987) Helix stabilization by Glu−···Lys+ salt bridges in short peptides of denovo design, *Proc. Natl. Acad. Sci. U.S.A. 84*, 8898−8902.
15. Jeffrey, G. A., and Saenger, W. (1994) in *Hydrogen Bonding in Biological Structures*, pp 365−371, Springer-Verlag, Heidelberg, Germany.
16. Anderson, D. E., Becktel, W. J., and Dahlquist, F. W. (1990) pH-Induced denaturation of proteins: a single salt bridge contributes 3−5 kcal/ mol to the free-energy of folding of T4-lysozyme, *Biochemistry 29*, 2403−2408.
17. Tissot, A. C., Vuilleumier, S., and Fersht, A. R. (1996) Importance of two buried salt bridges in the stability and folding pathway of barnase, *Biochemistry 35*, 6786−6794.
18. Milla, M. E., Brown, B. M., and Sauer, R. T. (1994) Protein stability effects of a complete set of alanine substitutions in Arc repressor, *Nat. Struct. Biol. 1*, 518−523.
19. Makhatadze, G. I., Loladze, V. V., Ermolenko, D. N., Chen, X. F., and Thomas, S. T. (2003) Contribution of surface salt bridges to protein stability: guidelines for protein engineering, *J. Mol. Biol. 327*, 1135−1148.
20. Horovitz, A., Serrano, L., Avron, B., Bycroft, M., and Fersht, A. R. (1990) Strength and cooperativity of contributions of surface salt bridges to protein stability, *J. Mol. Biol. 216*, 1031−1044.
21. Sali, D., Bycroft, M., and Fersht, A. R. (1991) Surface electrostatic interactions contribute little to stability of barnase, *J. Mol. Biol. 220*, 779−788.
22. Daopin, S., Sauer, U., Nicholson, H., and Matthews, B. W. (1991) Contributions of engineered surface salt bridges to the stability of T4 lysozyme determined by directed mutagenesis, *Biochemistry 30*, 7142−7153.
23. Munoz, V., and Serrano, L. (1995) Elucidating the folding problem of helical peptides using empirical parameters. 2. Helix macrodipole effects and rational modification of the helical content of natural peptides, *J. Mol. Biol. 245*, 275−296.
24. Fields, G. B., and Noble, R. L. (1990) Solid-phase peptide-synthesis utilizing 9-fluorenylmethoxycarbonyl amino-acids, *Int. J. Pept. Protein Res. 35*, 161−214.
25. Padmanabhan, S., York, E. J., Stewart, J. M., and Baldwin, R. L. (1996) Helix propensities of basic amino acids increase with the length of the side-chain, *J. Mol. Biol. 257*, 726−734.
26. Groebke, K., Renold, P., Tsang, K. Y., Allen, T. J., McClure, K. F., and Kemp, D. S. (1996) Template-nucleated alanine-lysine helices are stabilized by position-dependent interactions between the lysine side chain and the helix barrel, *Proc. Natl. Acad. Sci. U.S.A. 93*, 4025−4029.
27. Chou, P. Y., and Fasman, G. D. (1974) Conformational parameters for amino-acids in helical, β-sheet, and random coil regions calculated from proteins, *Biochemistry 13*, 211−222.
28. Scholtz, J. M., Qian, H., Robbins, V. H., and Baldwin, R. L. (1993) The energetics of ion-pair and hydrogen-bonding interactions in a helical peptide, *Biochemistry 32*, 9668−9676.
29. Huyghues-Despointes, B. M. P., Scholtz, J. M., and Baldwin, R. L. (1993) Helical peptides with 3 pairs of Asp-Arg and Glu-Arg residues in different orientations and spacings, *Protein Sci. 2*, 80−85.
30. Smith, J. S., and Scholtz, J. M. (1998) Energetics of polar side-chain interactions in helical peptides: salt effects on ion pairs and hydrogen bonds, *Biochemistry 37*, 33−40.
31. Merutka, G., Shalongo, W., and Stellwagen, E. (1991) A model peptide with enhanced helicity, *Biochemistry 30*, 4245−4248.
32. Merutka, G., and Stellwagen, E. (1991) Effect of amino-acid ion-pairs on peptide helicity, *Biochemistry 30*, 1591−1594.
33. Stellwagen, E., Park, S. H., Shalongo, W., and Jain, A. (1992) The contribution of residue ion-pairs to the helical stability of a model peptide, *Biopolymers 32*, 1193−1200.
34. Gans, P. J., Lyu, P. C., Manning, M. C., Woody, R. W., and Kallenbach, N. R. (1991) The helix-coil transition in heterogeneous peptides with specific side-chain interactions: theory and comparison with CD spectral data, *Biopolymers 31*, 1605−1614.
35. Lyu, P. C. C., Gans, P. J., and Kallenbach, N. R. (1992) Energetic contribution of solvent-exposed ion-pairs to α-helix structure, *J. Mol. Biol. 223*, 343−350.
36. Mayne, L., Englander, S. W., Qiu, R., Yang, J. X., Gong, Y. X., Spek, E. J., and Kallenbach, N. R. (1998) Stabilizing effect of a multiple salt bridge in a prenucleated peptide, *J. Am. Chem. Soc. 120*, 10643−10645.
37. Shi, Z. S., Olson, C. A., Bell, A. J., and Kallenbach, N. R. (2001) Stabilization of α-helix structure by polar side-chain interactions: complex salt bridges, cation-π interactions, and C-H···O H-bonds, *Biopolymers 60*, 366−380.
38. Olson, C. A., Spek, E. J., Shi, Z. S., Vologodskii, A., and Kallenbach, N. R. (2001) Cooperative helix stabilization by complex Arg-Glu salt bridges, *Proteins: Struct., Funct., Genet. 44*, 123−132.
39. Atherton, E., Fox, H., Harkiss, D., Logan, C. J., Sheppard, R. C., and Williams, B. J. (1978) Mild procedure for solid-phase peptide-synthesis: use of fluorenylmethoxycarbonylamino-acids, *J. Chem. Soc., Chem. Commun.* 537−539.
40. Edelhoch, H. (1967) Spectroscopic determination of tryptophan and tyrosine in proteins, *Biochemistry 6*, 1948−1954.
41. Pace, C. N., Vajdos, F., Fee, L., Grimsley, G., and Gray, T. (1995) How to measure and predict the molar absorption-coefficient of a protein, *Protein Sci. 4*, 2411−2423.
42. Lifson, S., and Roig, A. (1961) The theory of helix-coil transition in polypeptides., *J. Chem. Phys. 34*, 1963−1974.
43. Doig, A. J., Chakrabartty, A., Klingler, T. M., and Baldwin, R. L. (1994) Determination of free-energies of N-capping in α-helices by modification of the Lifson-Roig helix-coil theory to include N-capping and C-capping, *Biochemistry 33*, 3396−3403.
44. Chakrabartty, A., Kortemme, T., and Baldwin, R. L. (1994) Helix propensities of the amino-acids measured in alanine-based peptides without helix-stabilizing side-chain interactions, *Protein Sci. 3*, 843−852.
45. Chiu, H. P., Suzuki, Y., Gullickson, D., Ahmad, R., Kokona, B., Fairman, R., and Cheng, R. P. (2006) Helix propensity of highly fluorinated amino acids, *J. Am. Chem. Soc. 128*, 15556−15557.

46. Robert, C. H. (1990) A hierarchical nesting approach to describe the stability of α-helices with side-chain interactions, *Biopolymers 30*, 335−347.
47. Hobohm, U., and Sander, C. (1994) Enlarged representative set of protein structures, *Protein Sci. 3*, 522−524.
48. Kabsch, W., and Sander, C. (1983) Dictionary of protein secondary structure: pattern-recognition of hydrogen-bonded and geometrical features, *Biopolymers 22*, 2577−2637.
49. Efron, B., and Gong, G. (1983) A leisurely look at the bootstrap, the jackknife, and cross-validation, *Am. Stat. 37*, 36−48.
50. Kuebler, R. R., and Smith, H. (1976) *Statistics-A Beginning*, pp 302, John Wiley & Sons, New York.
51. Klugh, H. E. (1970) *Statistics-The Essentials for Research*, pp 350, John Wiley & Sons, New York.
52. Chakrabartty, A., Kortemme, T., Padmanabhan, S., and Baldwin, R. L. (1993) Aromatic side-chain contribution to far-ultraviolet circular-dichroism of helical peptides and its effect on measurement of helix propensities, *Biochemistry 32*, 5560−5565.
53. Chang, C. T., Wu, C. S. C., and Yang, J. T. (1978) Circular dichroic analysis of protein conformation: inclusion of the β-turns, *Anal. Biochem. 91*, 13−31.
54. Sali, D., Bycroft, M., and Fersht, A. R. (1988) Satbilization of protein structure by interaction of α-helix dipole with a charged side chain, *Nature 355*, 740−743.
55. Johnsson, K., Allemann, R. K., Widmer, H., and Benner, S. A. (1993) Synthesis, structure and activity of artificial, rationally designed catalytic polypeptides, *Nature 365*, 530−532.
56. McGregor, M. J., Islam, S. A., and Sternberg, M. J. E. (1987) Analysis of the relationship between side-chain conformation and secondary structure in globular-proteins, *J. Mol. Biol. 198*, 295−310.
57. Dunbrack, R. L., and Karplus, M. (1993) Backbone-dependent rotamer library for proteins, application to side-chain prediction, *J. Mol. Biol. 230*, 543−574.
58. Kemp, D. S., Oslick, S. L., and Allen, T. J. (1996) The structure and energetics of helix formation by short templated peptides in aqueous solution. 3. Calculation of the helical propogation constant *s* from the template stability constants t/c for Ac-Hel$_1$-Ala$_n$-OH, $n = 1-6$, *J. Am. Chem. Soc. 118*, 4249−4255.
59. Andrew, C. D., Penel, S., Jones, G. R., and Doig, A. J. (2001) Stabilizing nonpolar/polar side-chain interactions in the α-helix, *Proteins: Struct., Funct., Genet. 45*, 449−455.
60. Jeffrey, G. A., and Saenger, W. (1994) Chapter 7 Metrical Aspects of Two-Center Hydrogen Bonds, in *Hydrogen Bonding in Biological Structures*, pp 111−135, Springer-Verlag, Heildelberg, Germany.
61. Luo, P., and Baldwin, R. L. (1999) Interaction between water and polar groups of the helix backbone: an important determinant of helix propensities, *Proc. Natl. Acad. Sci. U.S.A. 96*, 4930−4935.
62. Garcia, A. E., and Sanbonmatsu, K. Y. (2002) α-Helical stabilization by side chain shielding of backbone hydrogen bonds, *Proc. Natl. Acad. Sci. U.S.A. 99*, 2782−2787.
63. Vu, C., Robblee, J., Werner, K. M., and Fairman, R. (2001) Effects of charged amino acids at b and c heptad positions on specificity and stability of four-chain coiled coils, *Protein Sci. 10*, 631−637.
64. Smith, C. K., and Regan, L. (1995) Guidelines for protein design: the energetics of β-sheet side-chain interactions, *Science 270*, 980−982.
65. Kiehna, S. E., and Waters, M. L. (2003) Sequence dependence of β-hairpin structure: comparison of a salt bridge and an aromatic interaction, *Protein Sci. 12*, 2657−2667.
66. Searle, M. S., Griffiths-Jones, S. R., and Skinner-Smith, H. (1999) Energetics of weak interactions in a β-hairpin peptide: electrostatic and hydrophobic contributions to stability from lysine salt bridges, *J. Am. Chem. Soc. 121*, 11615−11620.
67. Ciani, B., Jourdan, M., and Searle, M. S. (2003) Stabilization of β-hairpin peptides by salt bridges: role of preorganization in the energetic contribution of weak interactions, *J. Am. Chem. Soc. 125*, 9038−9047.
68. Searle, M. S. (2004) Insights into stabilizing weak interactions in designed peptide β-hairpins, *Biopolymers 76*, 185−195.
69. Cheng, R. P., and DeGrado, W. F. (2001) De novo design of a monomeric helical β-peptide stabilized by electrostatic interactions, *J. Am. Chem. Soc. 123*, 5162−5163.
70. Hart, S. A., Bahadoor, A. B. F., Matthews, E. E., Qiu, X. Y. J., and Schepartz, A. (2003) Helix macrodipole control of β^3-peptide 14-helix stability in water, *J. Am. Chem. Soc. 125*, 4022−4023.
71. Rueping, M., Mahajan, Y. R., Jaun, B., and Seebach, D. (2004) Design, synthesis and structural investigations of a β-peptide forming a 314-helix stabilized by electrostatic interactions, *Chem.−Eur. J. 10*, 1607−1615.
72. Altman, M., Lee, P., Rich, A., and Zhang, S. G. (2000) Conformational behavior of ionic self-complementary peptides, *Protein Sci. 9*, 1095−1105.
73. Hong, Y. S., Legge, R. L., Zhang, S., and Chen, P. (2003) Effect of amino acid sequence and pH on nanofiber formation of self-assembling peptides EAK16-II and EAK16-IV, *Biomacromolecules 4*, 1433−1442.
74. Kuehne, J., and Murphy, R. M. (2001) Synthesis and characterization of membrane-active GALA-OKT9 conjugates, *Bioconjugate Chem. 12*, 742−749.
75. Haas, D. H., and Murphy, R. M. (2004) Design of a pH-sensitive pore-forming peptide with improved performance, *J. Pept. Res. 63*, 9−16.
76. Haas, D. H., and Murphy, R. M. (2004) Templated assembly of the pH-sensitive membrane-lytic peptide GALA, *J. Pept. Res. 63*, 451−459.
77. Turk, M. J., Reddy, J. A., Chmielewski, J. A., and Low, P. S. (2002) Characterization of a novel pH-sensitive peptide that enhances drug release from folate-targeted liposomes at endosomal pHs, *Biochim. Biophys. Acta 1559*, 56−68.
78. Matsumura, S., Sakamoto, S., Ueno, A., and Mihara, H. (2000) Construction of α-helix peptides with β-cyclodextrin and dansyl units and their conformational and molecular sensing properties, *Chem.−Eur. J. 6*, 1781−1788.
79. Cline, D. J., Thorpe, C., and Schneider, J. P. (2004) Structure-based design of a fluorimetric redox active peptide probe, *Anal. Biochem. 325*, 144−150.

BI700701Z